

Critical chain length and superconductivity emergence in oxygen-equalized pairs of $\text{YBa}_2\text{Cu}_3\text{O}_{6.30}$

P. Manca and S. Sanna

Dipartimento di Fisica and Istituto Nazionale di Fisica della Materia (INFM), Università di Cagliari, Cittadella Universitaria, 09042 Monserrato (CA), Italy

G. Calestani

Dipartimento di Chimica Generale ed Inorganica, Chimica Analitica e Chimica Fisica, Università di Parma, Viale delle Scienze, 43100 Parma, Italy

A. Migliori

CNR-LAMEL, Area della Ricerca di Bologna, Via Gobetti 101, Bologna, Italy

R. De Renzi and G. Allodi

Dipartimento di Fisica and Istituto Nazionale di Fisica della Materia (INFM), Università di Parma, Viale delle Scienze 7a, 43100 Parma, Italy

(Received 19 July 1999)

The oxygen-order dependent emergence of superconductivity in $\text{YBa}_2\text{Cu}_3\text{O}_{6+x}$ is studied in a comparative way on pair samples having the same oxygen content and thermal history, but different $\text{Cu}(1)\text{O}_x$ chain arrangements deriving from their intercalated and deintercalated nature. Structural and electronic nonequivalence of pairs samples is detected in the critical region and found to be related, on microscopic scale, to a different average chain length, which, on being experimentally determined by nuclear quadrupole resonance (NQR), sheds light on the concept of critical chain length for hole doping efficiency.

The peculiarity of $\text{YBa}_2\text{Cu}_3\text{O}_{6+x}$ (123), the superconductor that still plays an important role in ongoing efforts to elucidate the mechanism of high- T_c superconductivity, is the existence of a charge reservoir, the $\dots\text{-Cu-O-Cu-}\dots$ chain system in the $\text{Cu}(1)\text{O}_x$ plane, far removed from the superconducting $\text{Cu}(2)\text{O}_2$ sheets. Its structural order drives the whole crystal structure in a variety of superstructures which have been observed¹⁻⁸ and modeled theoretically⁹⁻¹⁴ in the whole compositional x range. Beside the tetragonal (**T**, empty chain) and orthorhombic-I (**OI**, full chain) structures that characterize the end members of the compositional x range ($x=0$ and 1, respectively), at least two orthorhombic modifications, ortho-II (**OII**) and ortho-III (**OIII**), occurring around the ideal $x=0.5$ and $x=0.67$ compositions and characterized by a $\dots\text{-full-empty-}\dots$ and a $\dots\text{-full-full-empty-}\dots$ chain sequence along the a direction, are considered thermodynamically stable.^{8,9} The superstructures arising from an ordering between oxygen-poor and oxygen-rich chains are well described by a simple lattice-gas model, the asymmetric next-nearest-neighbor Ising model (ASYNNNI), introduced by de Fontaine *et al.*¹¹ Despite its simplicity the ASYNNNI model, which considers only second-nearest-neighbor interactions, can account for the stability region of the **OII** phase,¹⁵ for the thermodynamics,¹⁶ and for the oxygen ordering dynamics.¹⁷ Extensions of the model to include longer-range interactions¹² predict the occurrence of more complex superstructures (e.g., the **OIII** phase), even if they become significant only for very well equilibrated samples, as it was systematically verified¹⁸ in the range $0.63 \leq x \leq 0.75$.

The understanding of oxygen ordering in the $\text{Cu}(1)\text{O}_x$ plane and its effects on superconductivity in 123 systems has

been greatly enriched during the last 11 years. It is by now clearly established that the charge-transfer process in 123 systems and the related superconducting properties are a rather sensitive function not only of the oxygen content, but also of the oxygen ordering in the $\text{Cu}(1)\text{O}_x$ plane through its induced effects on hole density in the $\text{Cu}(2)\text{O}_2$ planes and consequently on T_c .^{19,20} The connection between oxygen ordering in the chains and hole behavior in the planes was already clearly manifested in the time-dependent increase of T_c during room-temperature annealing of samples produced by fast quenching.²⁰⁻²² The formation of the **OII** superstructure is responsible for the 60 K plateau typically observed in the T_c dependence from oxygen content in 123 and more recently the influence of **OIII** ordering on T_c has been shown.²³

The variety of possible superstructures has raised the question of the existence, for each different ordering scheme, of a characteristic T_c of their own.¹⁹ However, as stressed by Shaked *et al.*,²⁴ experiments that unambiguously prove this hypothesis are difficult or impossible as a result of the difficulty of stabilizing an entire sample in a particular ordered state and comparing such sample with those having the same oxygen content but a different ordering. The major limitation is the utilization of *single* samples, prepared one at a time in conditions that make a comparative study extremely difficult, owing to a lack in reproducibility produced by the significant influence of experimental conditions and thermal history on the 123 properties.

To investigate the effects of oxygen ordering we recently proposed a strategy based on oxygen-equalized pair samples,¹⁸ prepared simultaneously in the same thermal conditions, one by intercalation and the other by deintercalation

of oxygen, the fully oxygenated and reduced (**OI** and **T**) end terms of the $\text{YBa}_2\text{Cu}_3\text{O}_{6+x}$ system acting as oxygen donor and acceptor respectively, to arrive at the final oxygen content k in both samples. This topotacticlike technique for low-temperature processing of oxygen-equalized (k) deintercalated $[\text{D}]_k$ and intercalated $[\text{I}]_k$ pair samples of $\text{YBa}_2\text{Cu}_3\text{O}_{6+x}$ allowed us to investigate unanswered questions about the relationship between structure and superconductivity in this system.^{18,23} On the basis of the acquired experience in controlling the process reproducibility we are now able to explore, in comparative way, the most important (and at the same time the most difficult to study) region in the 123 system: the transient **T-O** boundary around $k = 0.30$, characterized by the vanishing of semiconducting antiferromagnetic (SAF) behavior and the emergence of superconductivity (SC).

Bulk polycrystalline $[\text{D}]_k$ and $[\text{I}]_k$ pair samples, hereafter referred to as k pairs, were prepared in a reproducible way starting with fully oxygenated **OI** bar-shaped samples of $(3.0 \times 2.0 \times 14.0) \text{mm}^3$, weighing each one about 0.5 g, prepared 20 at a time by following conventional solid-state reactions and sintering, and fully reduced **T** samples obtained from the former by dynamic vacuum annealing at 650°C . From iodometric and weight-loss analyses, the quoted oxygen content in the reference (**OI**, $x = 0.96$) and in the derived (**T**, $x = 0.07$) samples was estimated to be accurate within 0.02 oxygen atom per formula unit. Individually weighed **OI** and **T** bars were equilibrated at a given temperature (T_e) and order stabilized at composition-dependent temperatures (T_s) within the thermal stability domain of **OII** and **OIII** superstructures.^{25,26} By varying the **OI/T** mass ratios it is possible to prepare k -pairs in a wide range of equalized oxygen stoichiometry k . The **OI(T)** mass loss (gain) is due solely to a change in oxygen content in the $\text{Cu}(1)\text{O}_x$ plane,²⁷ and excellent agreement between calculated and experimental oxygen content at equilibrium was systematically obtained. Details on starting materials and k -pair processing were reported elsewhere.¹⁸ This topotacticlike procedure yields pairs of 123 specimens under equilibrium conditions with equal oxygen content and thermal history. The k pairs under investigation ($0.28 \leq k \leq 0.32$) were obtained by thermal equilibration of **OI** and **T** samples at $T_e = 670^\circ\text{C}$ for 1 day, slow cooling at $0.2^\circ\text{C}/\text{min}$ to $T_s = 75^\circ\text{C}$ followed by order stabilization at this temperature for 3 days and final cooling ($0.2^\circ\text{C}/\text{min}$) to room temperature. Several batches were prepared in this way and comparatively characterized by resistive ($\rho(T)$), electron diffraction (ED) and NQR studies.

Displayed in Fig. 1 are the evolution of the $\rho(T)$ curves (A) and the representative densitometer traces of an ensemble of ED patterns (B) recorded independently on several fragments of three typical samples. Panels 1 in Fig. 1 show the transport (A_1) and structural (B_1) characteristics of the $k = 0.28$ samples. Resistivity is thermally activated and only tetragonal peaks show up in the diffraction pattern. Both $[\text{I}]$ and $[\text{D}]$ are therefore characteristic of a nonsuperconducting tetragonal phase, for which $k = 0.28$ defines the upper limit of existence in both samples. Panels 4 likewise show the corresponding lower limit ($k = 0.32$) for the existence of a partially **OII**-ordered superconducting phase. Note the dif-

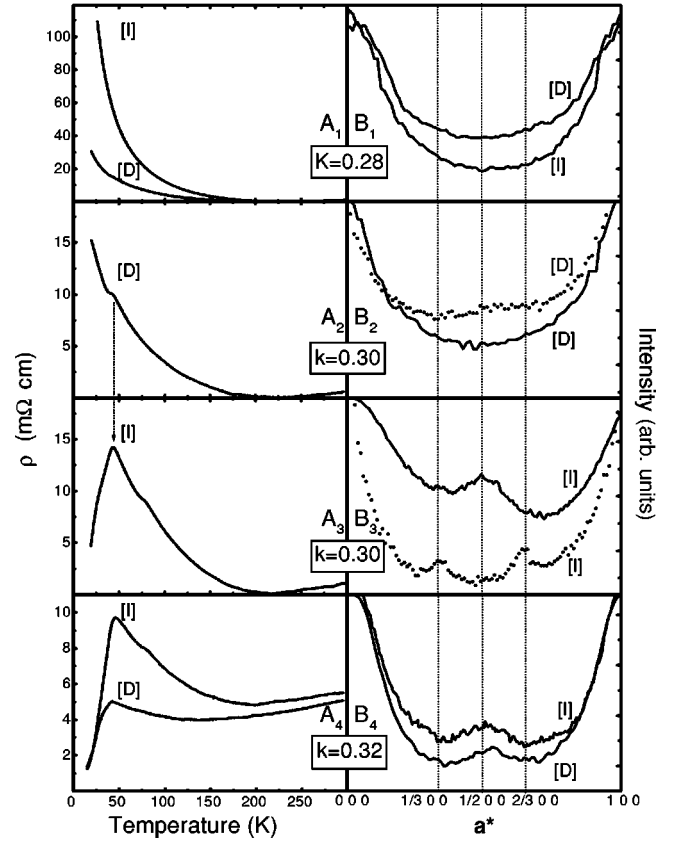


FIG. 1. Resistivity vs temperature (A) and representative densitometer traces of ED patterns along the a^* direction of the reciprocal lattice (B) for $[\text{D}]_k$ and $[\text{I}]_k$. Panel 1 and 4: data from $k = 0.28$ and $k = 0.32$ pairs, respectively; panel 2 and 3: $[\text{D}]$ and $[\text{I}]$ samples of a $k = 0.30$ pair.

fuse ($\frac{1}{2} 0 0$) peak in diffraction patterns B_4 [in agreement with the doubling of the a axis produced by a . . . -full-empty-. . . chain sequence in the $\text{Cu}(1)\text{O}_x$ plane] and the coincidence of T_c in the $[\text{I}]$ and $[\text{D}]$ curves A_4 . The situation is totally different in $k = 0.30$ pairs, which display a phase separation. Resistivity is shown in panels A_2 and A_3 . The $[\text{D}]$ sample is insulating, but its curve (A_2) displays a kink precisely at the same temperature where the corresponding $[\text{I}]$ sample shows (A_3 curve) the onset of the SC transition, which percolates the bar. $[\text{D}]$ grains invariably show the two kinds of patterns displayed in panel B_2 : most of them tetragonal (solid line) and a minority fraction **OII** (dotted line) characterized by very diffuse spots. A similar separation is observed for the $[\text{I}]$ samples: most grains are characterized by diffuse **OII** superstructure spots (solid line) or by diffuse (dotted line) extra peaks at $(h/3 0 0)$, whereas only few are tetragonal.

These data indicate that the **T-O** phase transition in the $k = 0.30$ pairs displays the coexistence of tetragonal and orthorhombic domains. This result is consistent with the prediction by de Fontaine *et al.*²⁸ from a lattice-gas model. However, the systematic observation of the $(h/3, 0 0)$ spots adds a new detail to this picture. We believe that these spots result from domains of an orthorhombic anti-III (**OIII***) structure characterized by an ideal . . . -empty-empty-full-. . . periodic arrangement of chains along the a direction.² Such a sequence gives rise to a tripling of the a

axis in analogy with the . . . -empty-full-full- . . . configuration for the ideal composition $x = \frac{2}{3}$ of the **OIII** superstructure.^{4,8} The **OIII*** structure is reproducibly observed around the ideal stoichiometry $x = \frac{1}{3}$ by means of our equilibration technique. After long-term aging (one year) of $[I]_{0.30}$ samples at room temperature the $(h/300)$ spots disappear, the original two-phase orthorhombic state (**OII** + **OIII***) stabilizes in the **OII** single-phase state and the resistive SC transition broadens considerably. Hence, the **OIII*** ordering appears to be a metastable precursor in the emergence of **OII** ordering in the $[I]_{0.30}$ SC samples.

The **OIII*** phase cannot be justified by the original ASYNNNI model,¹¹ due to the neglect of long-range interactions. These interactions were later introduced in an extended model,¹² limited to the $6.5 \leq x \leq 7$ range, to account for the observation of the **OIII** phase. Our carefully equilibrated samples, which reproducibly develop both the **OIII** ($k \sim 0.70$) (Ref. 18) and the **OIII*** ($k = 0.30$) phase, call for an extension of the long-range interaction models to the oxygen-poor region of the phase diagram.

We investigated the local structure by NQR to determine the degree of short-range order in $k = 0.3$ samples at the SAF-SC boundary.²⁹ The NQR resonance frequency, proportional to the electric-field gradient (EFG) at the nucleus, is characteristic of each distinct copper site in the lattice. Since there are two Cu isotopes (63 and 65) each lattice site gives rise to an isotope doublet, at fixed frequency ($\nu_{63}/\nu_{65} = 1.082$) and intensity ($I_{63}/I_{65} = 2.235$) ratios. The Cu NQR spectra of the pair $[D]_{0.30}$ and $[I]_{0.30}$ are plotted in Fig. 2 in the range 22–33 MHz, corrected for frequency-dependent sensitivity and relaxation. Each sample shows two isotope doublets, the solid line being the best Gaussian fit to the above-mentioned isotopic constraints. The EFG values of the two doublets identify them as two distinct Cu(1) sites:³⁰ the 28.05–30.35 MHz doublet is 2-Cu(1), linearly coordinated with apical oxygen and neighbored by oxygen vacancies (v -Cu¹⁺- v) in the plane, while the 22.1–23.9 MHz doublet corresponds to the chain-end configuration (O-Cu²⁺- v) of the threefold coordinated 3-Cu(1). The few 4-Cu(1) (O-Cu²⁺-O) contribute negligibly to the spectra because of their much larger EFG inhomogeneity.

The area A_i ($i = 2,3$) under each doublet yields the average number of oxygen atoms in the inter-Cu(1) sites (i.e., the average chain length) as $l = \frac{3}{7}(2A_2/A_3 + 1)$, and we obtain $l_I = 3.9(1)$ and $l_D = 1.9(1)$ for the two samples of the pair. The short average chain length found in $[D]_{0.30}$ is consistent with its broad NQR lines, since a short correlation length implies a broad distribution of EFG values. These results outline the role of the chain length in determining the chain hole-doping efficiency and confirm directly the theoretical

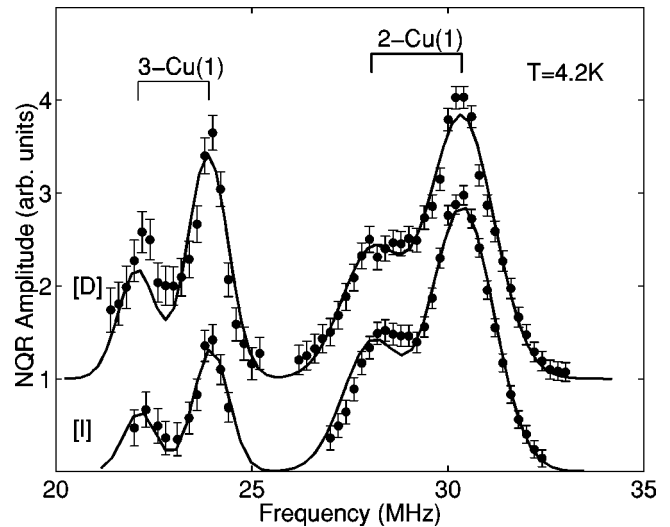


FIG. 2. NQR spectra of sample $[I]_{0.30}$ and $[D]_{0.30}$. The area under each isotope doublet, indicated as 3-Cu(1) and 2-Cu(1), respectively, is proportional to the number of Cu ions in that local environment.

prediction by Uimin *et al.*³¹ that there is essentially no charge transfer from chain fragments shorter than three oxygen atoms.

The k -pair method proves itself as an effective tool to extract more detailed information (inaccessible to *single sample* experiments) on the mechanism of short-range oxygen-chain ordering which characterizes the transient SAF-SC region. The experimentally demonstrated inequivalence of the $[D]_{0.30}$ and $[I]_{0.30}$ samples of a pair agrees with previous analogous results obtained around the **OII-OIII** and the **OIII-OI** transition boundaries.^{18,23} This leads us to conclude that different metastable states exist near the thermodynamic equilibrium at a given oxygen content and are connected with the vacancy ordering in the Cu(1)-O_x chain system. Different kinetic and thermodynamic reaction paths are realized during intercalation or deintercalation of oxygen and result in inequivalent chain growth processes revealed by ED and NQR. Moreover, we point out that with our equilibration scheme structurally distinct domains occur in the same sample in the transient region around $k = 0.3$, while the SC transition in $[I]_{0.30}$ and the resistive kink in $[D]_{0.30}$ (Fig. 1, A_2 - A_3) systematically occur at the same temperature. This suggests that a simultaneous electronic and structural phase separation takes place at the SAF-SC boundary, where orthorhombic (SC) and tetragonal (SAF) domains coexist. They originate nanoscopically and are critically dependent on the chain growth process. We believe that the different chain lengths observed in $[I]$ and $[D]$ samples represents an experimentally determined critical borderline between the vanishing of SAF behavior and the emergence of SC in 123.

¹M. A. Alario-Franco *et al.*, Physica C **156**, 455 (1988).

²J. Reyes-Gasga *et al.*, Physica C **159**, 831 (1989).

³C. J. Hou *et al.*, J. Mater. Res. **5**, 9 (1990).

⁴A. Stratilatov *et al.*, Phys. Lett. A **180**, 137 (1993).

⁵V. E. Zubkus, S. Lapinskas, A. Rosengren, and E. E. Tornau, Physica C **206**, 155 (1993).

⁶A. Stratilatov, V. Plakhty, Yu. Chernenkov, and V. Federov, Phys. Lett. A **180**, 137 (1993).

- ⁷V. Plakhty *et al.*, *Physica C* **235-240**, 867 (1994); F. Yakhou *et al.*, *ibid.* **261**, 315 (1996).
- ⁸P. Schleger *et al.*, *Physica C* **241**, 103 (1995).
- ⁹L. T. Wille, A. Berera, and D. de Fontaine, *Phys. Rev. Lett.* **60**, 1065 (1988).
- ¹⁰A. G. Khachaturyan and J. W. Morris, Jr., *Phys. Rev. Lett.* **61**, 215 (1988).
- ¹¹D. de Fontaine, L. T. Wille, and S. C. Moss, *Phys. Rev. B* **36**, 5709 (1987).
- ¹²G. Ceder, M. Asta, and D. de Fontaine, *Physica C* **177**, 106 (1991).
- ¹³H. F. Poulsen, N. H. Andersen, J. V. Andersen, H. Bohr, and O. G. Mouritsen, *Nature (London)* **349**, 594 (1991).
- ¹⁴A. A. Aligia and J. Garces, *Physica C* **194**, 223 (1992).
- ¹⁵J. Stolze, *Phys. Rev. Lett.* **64**, 970 (1990).
- ¹⁶V. E. Zubkus, E. E. Tornau, S. Lapinskas, and P. J. Kundrotas, *Phys. Rev. B* **43**, 13 112 (1991).
- ¹⁷H. F. Poulsen *et al.*, *Phys. Rev. Lett.* **66**, 465 (1991).
- ¹⁸P. Manca, P. Sirigu, G. Calestani, and A. Migliori, *Nuovo Cimento D* **19**, 1009 (1997).
- ¹⁹R. J. Cava *et al.*, *Physica C* **165**, 419 (1990).
- ²⁰J. D. Jorgensen *et al.*, *Physica C* **167**, 571 (1990).
- ²¹B. W. Veal *et al.*, *Phys. Rev. B* **42**, 6305 (1990).
- ²²B. W. Veal and A. P. Paulikas, *Physica C* **184**, 321 (1991).
- ²³G. Calestani, A. Migliori, P. Manca, and P. Sirigu, *Nuovo Cimento D* **19**, 1075 (1997).
- ²⁴H. Shaked, J. D. Jorgensen, D. G. Hinks, R. L. Hitterman, and B. Dabrowki, *Physica C* **205**, 225 (1993).
- ²⁵S. Yang *et al.*, *Physica C* **193**, 243 (1992).
- ²⁶P. Schleger *et al.*, *Physica C* **241**, 103 (1995).
- ²⁷J. D. Jorgensen *et al.*, *Phys. Rev. B* **36**, 3608 (1987).
- ²⁸D. de Fontaine, G. Ceder, and M. Asta, *Nature (London)* **343**, 544 (1990).
- ²⁹S. Sanna, Degree thesis, University of Cagliari, 1998.
- ³⁰H. Lütgemeier *et al.*, *Physica C* **267**, 191 (1996).
- ³¹G. V. Uimin *et al.*, *Physica C* **192**, 481 (1992).